

## Role of actin microfilaments in phragmoplast guidance to the cortical division zone

Toshio Sano<sup>1,\*</sup>, Tomomi Hayashi<sup>2</sup>, Natsumaro Kutsuna<sup>2</sup>, Toshiyuki Nagata<sup>1</sup>  
and Seiichiro Hasezawa<sup>2,3</sup>

<sup>1</sup>Faculty of Bioscience and Applied Chemistry, Hosei University, E5003, 3-7-2, Kajinocho, Koganeishi, Tokyo 184-8584, <sup>2</sup>Graduate School of Frontier Sciences, The University of Tokyo, Kashiwashi, Chiba 277-8562, <sup>3</sup>Advanced Measurement and Analysis, Japan Science and Technology Agency (JST), Chiyodaku, Tokyo 102-0076, Japan

### ABSTRACT

Actin microfilaments are cytoskeletal structures that constitute the major cytoskeleton in higher plant cells and are often considered to co-localize with microtubule structures. In this study, we observed the interaction of actin microfilaments and microtubules in transgenic tobacco BY-2 cells, dual-visualizing these two cytoskeletal structures using fluorescent protein-labeled cytoskeletal marker proteins. In combination with pharmacological studies, we focused on the role of actin microfilaments in phragmoplast guidance to the proper cortical division zone (CDZ) and discuss their role in increasing the chance to meet the CDZ, to recognize the CDZ, and to guide microtubules to the CDZ.

**KEYWORDS:** actin microfilament, microtubule, phragmoplast, tobacco BY-2 cell

### ABBREVIATIONS

actin microfilaments (AFs), bistheonellide A (BA), cortical division zone (CDZ), microtubules (MTs), preprophase band (PPB)

### INTRODUCTION

Actin microfilaments (AFs) are major cytoskeletons in higher plant cells and are involved in diverse

cellular activities, such as cellular morphogenesis, cytoplasmic streaming and intracellular transport [1, 2]. In addition to these major cytoskeletons, microtubules (MTs) constitute four typical structures during the plant cell cycle progression; the cortical microtubules in G<sub>1</sub> phase, the preprophase band (PPB) in late G<sub>2</sub> phase, the mitotic spindle in metaphase and the phragmoplast in telophase [3, 4]. AFs and MTs are often observed to co-localize, and pharmacological analyses have suggested an interaction between the two [5, 6, 7].

The phragmoplast is a plant-specific cytokinetic apparatus consisting of MTs, AFs and endoplasmic reticulum (ER) [8]. After chromosome separation, the phragmoplast appears, grows centrifugally between the separated chromosomes and the growing edge of the phragmoplast reaches the parental cell wall that had once been occupied by the PPB. This membrane domain once occupied by PPB has recently been referred to as the cortical division zone (CDZ) [8, 9]. Finally, the phragmoplast guides the cell plate to the site of the cell cortex, which has also recently been referred to as the cortical division site (CDS) [10, 11]. The CDZ was once determined by localization of the PPB in G<sub>2</sub> phase, however, the mechanism of the memory is still in debate since the PPB is disassembled in mitosis [10, 11, 12, 13]. After the disappearance of the PPB, as a region with a low intensity of AFs appears where

---

\*Corresponding author:  
toshiosano@hosei.ac.jp

the PPB once existed, AFs have been considered to be members that determine and maintain the CDZ [7, 14]. The region is thus referred to as the actin-depleted zone (ADZ) [15, 16] or microfilament twin-peaks (MFTP) [14].

In this study, we observed the interaction of AFs and MTs in transgenic tobacco BY-2 cells by dual-visualizing these two cytoskeletal structures using fluorescent protein-labeled cytoskeletal marker proteins. Previously, the microtubule-end binding protein (EB) 1 was used to decorate the MT plus-ends in addition to the growing MTs [17, 18], whereas the actin binding domain (ABD) of fimbrin was used to label the AFs [14, 19]. In a recent report, MTs and AFs were similarly dual-visualized using the fluorescent-labeled marker proteins of tubulin and ABD in *Arabidopsis* hypocotyl cells [20]. These latter pharmacological studies, using the actin-depolymerizing drug latrunculin B and the actin-stabilizing drug jasplakinolide, suggested a role of MTs in the orientation of newly-formed AFs, and a role of AFs in actin assembly or turnover in MT orientation [20]. In this current study, we focus on the role of AFs in MT structural formation by visualizing the growing tips of MTs. We therefore discuss the role of AFs in phragmoplast guidance to the CDZ.

## MATERIALS AND METHODS

### Plant material

Tobacco BY-2 (*Nicotiana tabacum* L. cv. Bright Yellow 2) suspensions were diluted 95-fold with a modified Linsmaier and Skoog medium supplemented with 2,4-D (LSD) at weekly intervals, as described in [21]. The cell suspensions were agitated on a rotary shaker at 130 rpm at 27°C in the dark. Cell synchronization was performed as described in [22]. In brief, 10 ml of 7-d old cells were transferred to 95 ml fresh medium and cultured for 24 h with 5 mg liter<sup>-1</sup> aphidicolin (Sigma, St Louis, MO, USA). The cells were washed with 10 volumes of fresh medium and then resuspended in the same medium.

### Construction of RFP-EB1

The ORF regions of TagRFP [23, 24] and *Arabidopsis* EB1B (At5g62500) [18] were PCR

amplified and the fragments used to replace the sGFP (S65T)-fimbrin ABD2 region of CaMV35S-sGFP (S65T)-fimbrin ABD2 in pUC18 vector [14], resulting in an in-frame fusion of the N-terminus TagRFP and C-terminus EB1 under the control of the 35S promoter. The resulting 35S-TagRFP-EB1 region was then subcloned into the binary vector pCAMBIA2300 (CAMBIA, Canberra, Australia) for transformation.

### Transformation and establishment of tobacco BY-2 stably expressing the RFP-EB1 fusion protein

Tobacco BYGF cells, in which actin microfilaments were GFP-labeled [14], were transformed with the TagRFP-EB1 construct. Here, the construct was first transformed into *Agrobacterium tumefaciens* strain, LBA4404, and a 100 µl aliquot of an overnight culture of this strain then was incubated with 4 ml of 2-d old tobacco BYGF cells as described by [25]. After 2 d of incubation at 27°C, the cells were washed 4 times in 15 ml LSD medium, and then plated onto solid LSD medium containing 500 mg liter<sup>-1</sup> carbenicillin and 50 mg liter<sup>-1</sup> kanamycin. Calluses, which appeared after 6 to 8 weeks, were transferred onto new plates and cultured independently until they reached about 1 cm in diameter, when they were transferred to 20 ml liquid LSD medium and agitated on a rotary shaker at 130 rpm at 27°C in the dark. Cell lines suitable for observing RFP-EB1 fluorescence were selected by fluorescent microscopy and the obtained cell line then designated as BY-GFRE.

### Microscopy

For time-sequential observations, synchronized BY-GFRE cells were transferred into ø35 mm Petri dishes with ø14 mm coverslip windows at the bottom (Matsunami Glass Ind. Ltd., Osaka, Japan). The dishes were placed onto the inverted platform of a fluorescence microscope equipped with a spinning disc confocal laser scanning system (CSU X1, Yokogawa, Tokyo, Japan) and a cooled CCD camera (Cool-SNAP HQ, PhotoMetrics, Huntington Beach, Canada).

Cell plates were observed after staining the cells with *N*-(3-triethylammoniumpropyl)-4-(6-(4-(diethylamino) phenyl) hexatrienyl) pyridinium dibromide (FM4-64; Molecular Probes, Invitrogen) as described [26].

## RESULTS

### EB1 proteins do not move along with actin microfilaments on the cell surface

To observe the interaction of microtubules (MTs) and actin microfilaments (AFs) in living cells, a transgenic tobacco BY-2 cell line was prepared that stably expressed RFP-EB1 and GFP-ABD2. The EB1 proteins were found to decorate the MT plus-ends in addition to the growing MTs [17, 18], whereas ABD2 from *Arabidopsis* AtFim1 labeled the AFs [14, 19]. In this cell line, named tobacco BY-GFRE (BY-2 GFP-Fimbrin RFP-EB1), the MTs and AFs can be dual-visualized in living cells during standard cell cycle progression after cell synchronization with aphidicolin [22]. In S phase cells, cortical MTs and AFs developed and these structures could be observed in one optical plane (about 0.8  $\mu\text{m}$  depth, Figure 1). However, the EB1 fluorescence did not necessarily localize with the AFs when the images were merged (Figure 1F). In contrast, in the cytoplasmic strands, the EB1 fluorescence largely localized along with the AFs (Figure 1E).

During  $G_2$  phase progression, the MTs formed a preprophase band (PPB) in the middle of the cells (Figure 2C and D). At this stage, the cortical AFs were predominantly transverse-oriented and formed a band-like structure similar to the MT PPB (Figure 2B) [14]. The actin band was found to be broader than the MT PPB (Figure 2F), and concurred with previously demonstrated results from immuno-fluorescent microscopy [4]. Images obtained from the midplane of the cell showed that while the MT PPB was localized near the cell cortex, the AFs were on a relatively inner side of the cortex (Figure 2E). Between the cell cortex and the cell nuclei, AFs were localized to a cytoplasmic-rich region known as the phragmosome (Figure 2A) [7]. When we focused on the cytoplasmic strands in early  $G_2$  phase cells, a time-sequential observation showed that the EB1 fluorescence moved from the nuclear surface to the cell cortex along with the cytoplasmic AFs (Figure 3).

In metaphase cells, the MTs and AFs did not co-localize well, with the MTs forming the mitotic spindle and the AFs forming cortical structures called the microfilament-twin peaks (MFTP) [14]

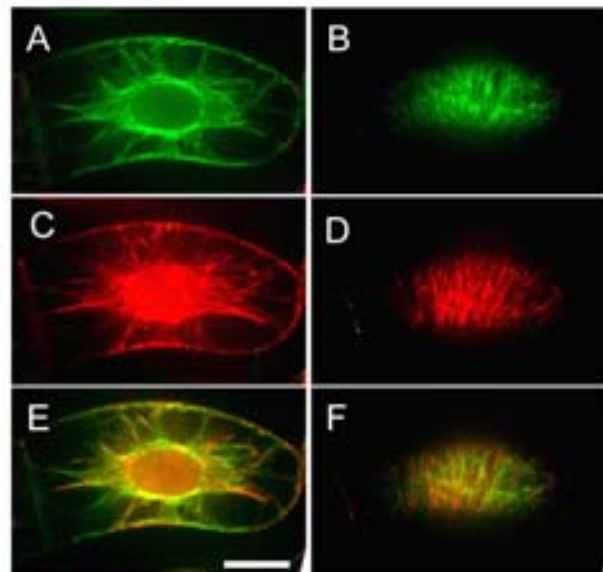


**Figure 1.** Actin microfilament and EB1 localization in an S phase BY-GFRE cell. Actin microfilaments (A and B) and EB1 (C and D) were dual-visualized in an S phase cell at the cell midplane (A and C) and at the cell cortex (B and D). Merged images of A plus C and B plus D are shown, respectively with the merged pixels shown in yellow (E and F). The scale bar represents 20  $\mu\text{m}$ .

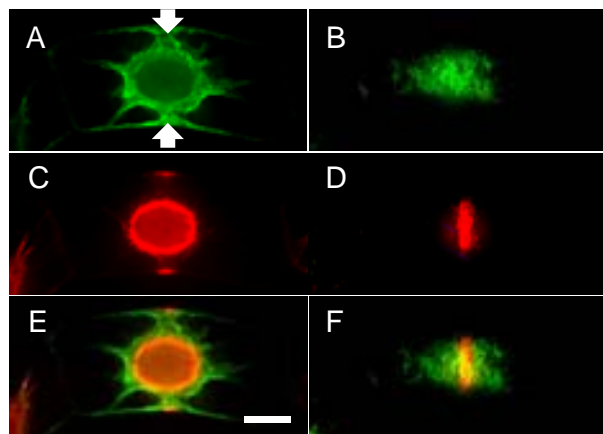


**Figure 2.** Actin microfilament and EB1 localization in a late  $G_2$  phase BY-GFRE cell. Actin microfilaments (A and B) and EB1 (C and D) were dual-visualized in a late  $G_2$  phase cell at the cell midplane (A and C) and the cell cortex (B and D). Merged images of A plus C and B plus D are shown, respectively with the merged pixels shown in yellow (E and F). Arrows in (A) indicate the phragmosome region. The scale bar represents 20  $\mu\text{m}$ .

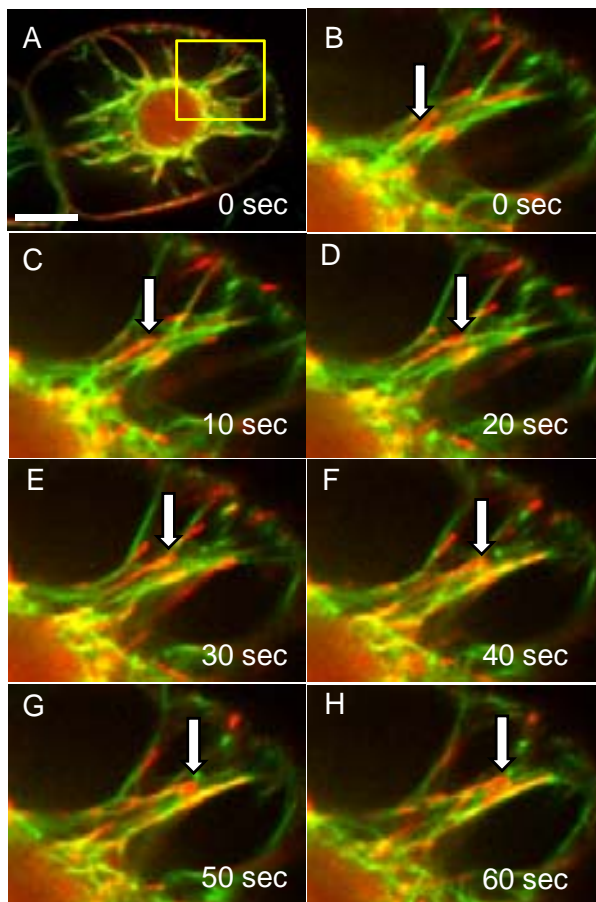


**Figure 3.** EB1 movement along with actin microfilaments. (A) A BY-GFRE cell in G<sub>2</sub> phase. (B) to (H): Dynamics of actin microfilaments (green) and EB1 (red) time-sequentially observed and shown at 10 sec. intervals in the boxed region of (A). The arrow indicates one particular RFP-EB1 fluorescence. The scale bar represents 20  $\mu$ m.

or the actin-depleted zone (ADZ) [16] (Data not shown).

### Actin microfilament dynamics during phragmoplast growth

At telophase, the MTs and AFs were largely colocalized in the phragmoplast that formed between the separated chromosomes (Figure 4A). At the tip of the growing edge, the AFs elongated to the cell surface and finally associated with those from the cell surface (Figure 4A). In a close view of the growing edge, the newly forming MTs seemed to elongate along the AFs as they did in the cytoplasmic strands (Figure 4B).

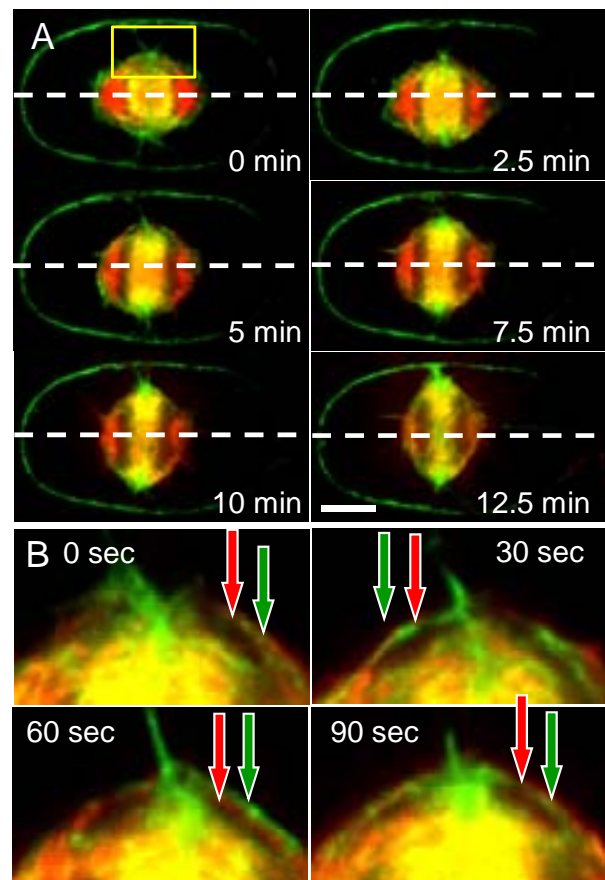


**Figure 4.** Dynamics of actin microfilaments and EB1 during phragmoplast growth. (A) Dynamics of actin microfilaments (green) and microtubules (red) were time-sequentially observed and the images shown at 2.5 min. intervals. The dashed lines indicate the mid-plane of the images. The scale bar represents 20  $\mu$ m. (B) Close view of the phragmoplast growing edge boxed in (A). Images are shown at 30 sec. intervals. Green and red arrows indicate the actin microfilaments and EB1, respectively.

During phragmoplast growth, time-sequential observations revealed its growth with concomitant vibrations (Figure 4A). Disruption of the AF structures by treatment with 1  $\mu$ M bistheonellide A (BA), an actin polymerization inhibitor, terminated the vibrations but did not arrest phragmoplast formation (Data not shown). In some cells, the phragmoplast was found to be inclined towards the future cell plate orientation. However, the inclination gradually decreased during phragmoplast growth and the AFs at the phragmoplast edge finally associated with those

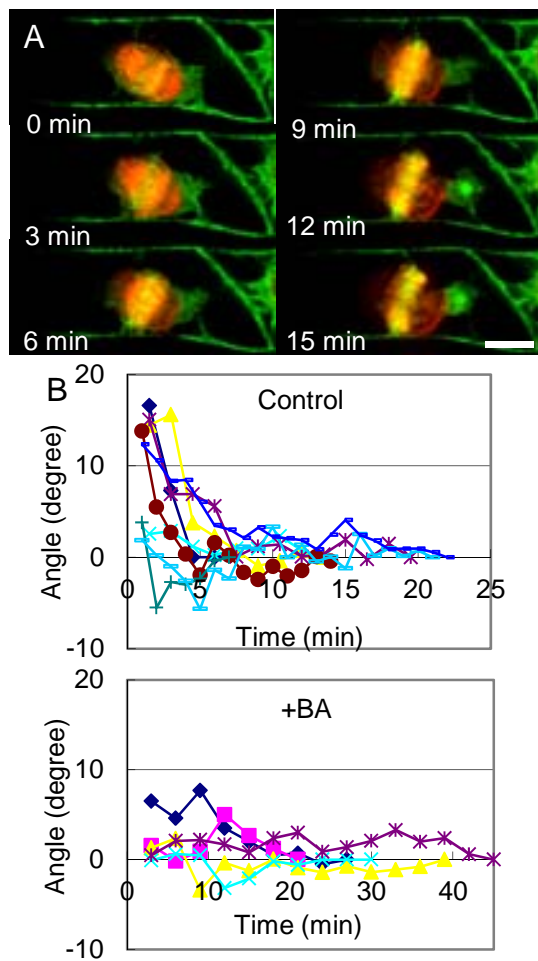


**Figure 5.** Reorientation of an inclined phragmoplast. (A) A BY-GFRE cell in telophase was time-sequentially observed and the images shown at 3 min. intervals. Actin microfilaments and EB1 are shown in green and red, respectively. The scale bar represents 20  $\mu\text{m}$ . (B) Changes in the angle of the cell plate. Cell plates were stained with FM4-64 and the inclination of the cell plate then measured time-sequentially. In the control (Control) and BA treated condition (+BA), data from 8 and 5 cells were plotted, respectively.

from the cell cortex (Figure 5A). When we monitored the changes in cell plate inclination in the phragmoplast, several cells under control conditions had cell plates with inclinations of nearly 15 degrees to the future cell division plane, with the inclination gradually decreasing to 0 degrees in 20 min (Figure 5B). In BA treated cells, the inclination was about 5 degrees at the start of phragmoplast formation, and took nearly 40 min to return back to 0 degrees (Figure 5B).

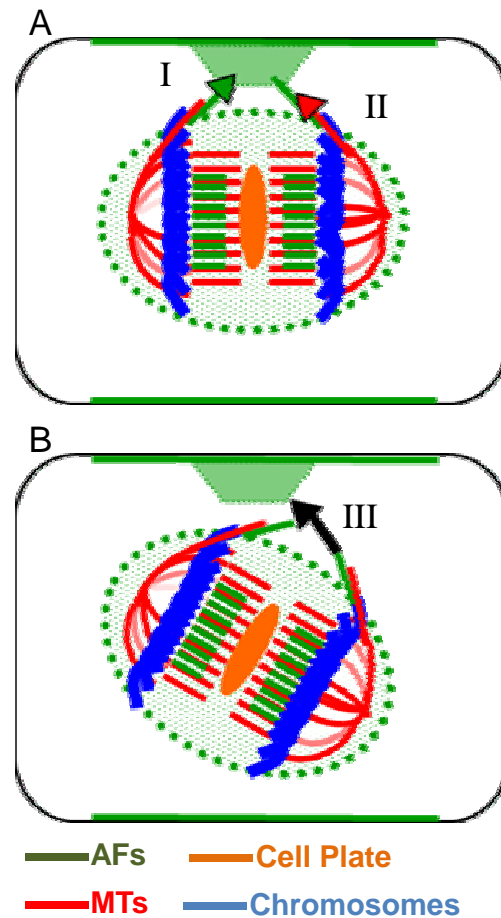


**Figure 6.** A predicted model for the role of actin microfilaments in phragmoplast guidance. (A) Actin microfilaments (AFs) at the phragmoplast growing edge elongate to the cell cortex and associate with those from the cell cortex (green arrow I). Along the AF orientation, microtubules elongate to the CDZ marked on the cell cortex (red arrow II). (B) Vibrations of the phragmoplast increase the chances of the AFs at the growing edge of the inclined phragmoplast meeting with those from the cell cortex (black arrow III).

## DISCUSSION

### Role of actin microfilaments in phragmoplast guidance to the cortical division zone

In this paper, we have demonstrated the role of AFs in guiding the phragmoplast to the cortical cell division zone. In our model, the AFs at the edge of the phragmoplast first elongate to the cell surface and associate with those that elongated from the CDZ (Figure 6A I). Then, the MTs at the phragmoplast edge elongate to the cell surface

along with the AFs (Figure 6A II). The determination of MT orientation by AF elongation would decide the position of the cell plate to the CDZ. In addition, in some cells, the phragmoplast starts to grow with an inclination towards the future cell plate orientation. The vibrations observed during phragmoplast growth may increase the chance of AFs at the phragmoplast edge meeting with those from the CDZ (Figure 6B III).

Concerning the association of AFs, recent reports have demonstrated that AF-bundling is assisted by actin-binding proteins, such as villin and LIM proteins [27, 28, 29]. In particular, *Arabidopsis* VILLIN1 and VILLIN3 have been shown to induce AF-bundling by a 'catch and zipper' mechanism in which AFs positioned close to each other make contact and zipper together to form AF bundles [27]. In our study, although the kinds of actin-binding proteins involved have not yet been clarified, such bundling may guide MT elongation at the growing edge of the phragmoplast. Another possibility may be that the AF bundles provide cytoplasmic-rich regions, similar to the cytoplasmic strands [30], in which the phragmoplast and cell plate could grow to the cell cortex.

With MT elongation along the AF orientation, cross-linking proteins between the AFs and MTs may mediate its elongation. Such candidate cross-linking proteins could be microtubule-associated proteins (MAPs), formins or kinesins with the calponin-homology domain [31, 32, 33]. A microtubule-associated 190 kDa protein, MAP190, from tobacco cells was also found to bind AFs and was suggested to play a role in proper cell division [34]. Recent studies have also indicated the possible functions of formins as linking proteins between MTs and AFs [35, 36, 37]. Among these, the *Arabidopsis* formin AFH14 was detected in the phragmoplast and implicated to play roles in cell division [38]. However, the role of these proteins in proper cell plate guidance has not yet been clarified. Another possibility would be that, although RFP-EB1 fluorescence was detected very close to the AFs, the MTs and AFs are not necessarily connected by cross-linking proteins. In this case, AFs may just provide a cytoplasm-rich region in which the MTs could

self-organize and elongate. MTs themselves have been suggested to interact with a positive CDZ marker, TANGLED [11, 39], and thus they may guide the phragmoplast to the CDZ.

In deciding the CDZ, an interesting example is the negative CDZ marker, kinesin KCA1 [40]. At the region where KCA1 proteins are depleted, the plasma membrane and cell wall are connected [40]. Removal of membrane proteins by endocytosis has been found to keep the positional memory established by the PPB [41, 42].

The phragmoplast vibrations could be driven by the AF themselves since disruption of AF structures by bistheonellide A treatment arrested the vibrations and increased the period needed to decrease phragmoplast inclination (Figure 5B). In leek (*Allium porrum* L.) leaf epidermal cells, cortical microtubules reoriented developmentally from the transverse to longitudinal directions driven by actomyosin-dependent cytoplasmic streaming [43]. Furthermore, ER motility, in addition to actin and myosins, has been suggested to cause cytoplasmic hauling, traditionally defined as cytoplasmic streaming [44]. In addition to these observations, AF movement itself would generate phragmoplast vibrations through cytoplasmic streaming.

### **Cortical microtubule elongation does not correlate with actin microfilaments**

At the cell cortex, previous immuno-cytochemical observations demonstrated the co-localization of MTs and AFs and suggested a role of cortical AFs in the decision of cortical MT orientation [5]. Recent dual-visualizations of MTs and AFs by fluorescent proteins also support the partial and temporal co-localization of these two structures at the cell cortex [20, 45]. In our observations, however, the EB1 fluorescence did not necessarily move along with the AFs at the cell cortex (Figure 1). In addition, the cortical MTs localized rather near the cell cortex whereas the AFs were in the cytoplasm (Figure 2). The localization of the FH1FH2 domain of *Arabidopsis* AFH14 and of tobacco kinesin NtKCH to the cortical MTs but not to the AFs in non-dividing onion cells or tobacco BY-2 cells [46, 47] support our observations. These discrepancies may be explained by the possibility that MTs could elongate without

the help of AFs but that MT arrangement requires the AF activities. Recent computer simulations of cortical MT arrangement have suggested that MTs could self-order into parallel arrays by MT interactions and potential depolymerization called 'catastrophe' [48, 49, 50]. AFs may therefore be involved in cortical MT arrangement through, for example, modification of the initial MT localization or the ratio of catastrophe.

In contrast, the EB1 fluorescence appears to move very closely along with the AFs in the cytoplasmic strands (Figure 3). Similar colocalization of MTs and AFs has been observed in *Arabidopsis* formin AFH14 and tobacco kinesin NtKCH in phragmoplasts [38, 47]. Therefore, in our observations, the MTs are structures that are largely associated with AFs in the cytoplasm but not to any great extent in the cell cortical region. These differential interactions may be regulated by the activity of the MT-AF linking proteins, although regulation of this linking-protein activity has not yet been clarified.

## CONCLUSIONS

In this study, we have suggested three different possible roles of AFs in phragmoplast guidance. First, in increasing the chance to meet the CDZ; second, in recognizing the CDZ; and thirdly, in guiding the MTs to the CDZ. In addition to examining the role of cytoskeletons, elucidating the functions of cytoskeletal-associated proteins and membrane trafficking would further clarify what decides the CDZ in relation to PPB localization, the long-standing question.

## ACKNOWLEDGMENTS

We thank Dr. Jaideep Mathur for the *Arabidopsis* EB1B construct. This work was financially supported in part by a Grant-in-Aid for Scientific Research on Priority Areas to S.H. (No. 23012009), a Grant-in-Aid for Scientific Research on Innovative Areas to S.H. (No. 22114505) from the Japanese Ministry of Education, Science, Culture, Sports and Technology, an Advanced Measurement and Analysis grant from the Japan Science and Technology Agency (JST) to S.H. and the Wada Kunkokai Foundation, Japan to T.S.

## REFERENCES

1. Petrášek, J. and Schwarzerová, K. 2009, *Curr. Opin. Plant Biol.*, 12, 728.
2. Higaki, T., Kojo, K. H. and Hasezawa, S. 2010, *Plant Signal. Behav.*, 5, 484.
3. Zhang, D., Wadsworth, P. and Hepler, P. K. 1990, *Proc. Natl. Acad. Sci. USA*, 87, 8820.
4. Hasezawa, S., Marc, J. and Palevitz, B. A. 1991, *Cell Motil. Cytoskeleton*, 18, 94.
5. Hasezawa, S., Sano, T. and Nagaga, T. 1998, *Protoplasma*, 202, 105.
6. Blancaflor, E. B. 2000, *J. Plant Growth Regul.*, 19, 406.
7. Hoshino, H., Yoneda, A., Kumagai, F. and Hasezawa, S. 2003, *Protoplasma*, 222, 157.
8. Müller, S. 2012, *Protoplasma*, 249, 239.
9. Van Damme, D., Gadeyne, A., Vanstraelen, M., Inzé, D., Van Montagu, M. C., De Jaeger, G., Russinova, E. and Geelen, D. 2011, *Proc. Natl. Acad. Sci. USA*, 108, 615.
10. Duroc, Y., Bouchez, D. and Pastuglia, M. 2011, Liu, B. (Ed.), in *The Plant Cytoskeleton*, pp145.
11. Rasmussen, C. G., Sun, B. and Smith, L. G. 2011, *J. Cell Sci.*, 124, 270.
12. Panteris, E. 2008, *New Phytol.*, 179, 334.
13. Müller, S., Wright, A. J. and Smith, L. G. 2009, *Trends Cell Biol.*, 19, 180.
14. Sano, T., Higaki, T., Oda, Y., Hayashi, T. and Hasezawa, S. 2005, *Plant J.*, 44, 595.
15. Cleary, A. L., Gunning, B. E. S., Wasteneys, G. O. and Hepler, P. K. 1992, *J. Cell Sci.*, 103, 977.
16. Liu, B. and Palevitz, B. A. 1992, *Cell Motil. Cytoskeleton*, 23, 252.
17. Chan, J., Calder, G. M., Doonan, J. H. and Lloyd, C. W. 2003, *Nat. Cell Biol.*, 5, 967.
18. Mathur, J., Mathur, N., Kernebeck, B., Srinivas, B. P. and Hülskamp, M. 2003, *Curr. Biol.*, 13, 1991.
19. Sheahan, M. B., Rose, R. J. and McCurdy, D. W. 2004, *Plant J.*, 37, 379.
20. Sampathkumar, A., Lindeboom, J. J., Debolt, S., Gutierrez, R., Ehrhardt, D. W., Ketelaar, T. and Persson, S. 2011, *Plant Cell*, 23, 2302.
21. Nagata, T., Nemoto, Y. and Hasezawa, S. 1992, *Int. Rev. Cytol.*, 132, 1.

22. Kumagai-Sano, F., Hayashi, T., Sano, T. and Hasezawa, S. 2006, *Nat. Protoc.*, 1, 2621.
23. Merzlyak, E. M., Goedhart, J., Shcherbo, D., Bulina, M. E., Shcheglov, A. S., Fradkov, A. F., Gaintzeva, A., Lukyanov, K. A., Lukyanov, S., Gadella, T. W. and Chudakov, D. M. 2007, *Nat. Methods*, 4, 555.
24. Shaner, N. C., Lin, M. Z., McKeown, M. R., Steinbach, P. A., Hazelwood, K. L., Davidson, M. W. and Tsien, R. Y. 2008, *Nat. Methods*, 5, 545.
25. Mayo, K. J., Gonzales, B. J. and Mason, H. S. 2006, *Nat. Protoc.*, 1, 1105.
26. Higaki, T., Kutsuna, N., Sano, T. and Hasezawa, S. 2008, *BMC Plant Biol.*, 8, 80.
27. Khurana, P., Henty, J. L., Huang, S., Staiger, A. M., Blanchoin, L. and Staiger, C. J. 2010, *Plant Cell*, 22, 2727.
28. Papuga, J., Hoffmann, C., Dieterle, M., Moes, D., Moreau, F., Tholl, S., Steinmetz, A. and Thomas, C. 2010, *Plant Cell*, 22, 3034.
29. Zhang, H., Qu, X., Bao, C., Khurana, P., Wang, Q., Xie, Y., Zheng, Y., Chen, N., Blanchoin, L., Staiger, C. J. and Huang, S. 2010, *Plant Cell*, 22, 2749.
30. Higaki, T., Kutsuna, N., Okubo, E., Sano, T. and Hasezawa, S. 2006, *Plant Cell Physiol.*, 47, 839.
31. Hamada, T. 2007, *J. Plant Res.*, 120, 79.
32. Frey, N., Klotz, J. and Nick, P. 2010, *J. Exp. Bot.*, 61, 3423.
33. Wang, J., Xue, X. and Ren, H. 2012, *Protoplasma*, 249, S101.
34. Igarashi, H., Orii, H., Mori, H., Shimmen, T. and Sonobe, S. 2000, *Plant Cell Physiol.*, 41, 920.
35. Deeks, M. J., Fendrych, M., Smertenko, A., Bell, K. S., Oparka, K., Cvrcková, F., Zársky, V. and Hussey, P. J. 2010, *J. Cell Sci.*, 123, 1209.
36. Yang, W., Ren, S., Zhang, X., Gao, M., Ye, S., Qi, Y., Zheng, Y., Wang, J., Zeng, L., Li, Q., Huang, S. and He, Z. 2011, *Plant Cell*, 23, 661.
37. Zhang, Z., Zhang, Y., Tan, H., Wang, Y., Li, G., Liang, W., Yuan, Z., Hu, J., Ren, H. and Zhang, D. 2011, *Plant Cell*, 23, 681.
38. Li, Y., Shen, Y., Cai, C., Zhong, C., Zhu, L., Yuan, M. and Ren, H. 2010, *Plant Cell*, 22, 2710.
39. Walker, K. L., Müller, S., Moss, D., Ehrhardt, D. W. and Smith, L. G. 2007, *Curr. Biol.*, 17, 1827.
40. Vanstraelen, M., Van Damme, D., De Rycke, R., Mylle, E., Inzé, D. and Geelen, D. 2006, *Curr. Biol.*, 16, 308.
41. Dhonukshe, P., Mathur, J., Hülskamp, M. and Gadella, T. W. Jr. 2005, *BMC Biol.*, 3, 11.
42. Karahara, I., Suda, J., Tahara, H., Yokota, E., Shimmen, T., Misaki, K., Yonemura, S., Staehelin, L. A. and Mineyuki, Y. 2009, *Plant J.*, 57, 819.
43. Sainsbury, F., Collings, D. A., Mackun, K., Gardiner, J., Harper, J. D. and Marc, J. 2008, *Plant J.*, 56, 116.
44. Ueda, H., Yokota, E., Kutsuna, N., Shimada, T., Tamura, K., Shimmen, T., Hasezawa, S., Dolja, V. V. and Hara-Nishimura, I. 2010, *Proc. Natl. Acad. Sci USA*, 107, 6894.
45. Buschmann, H., Green, P., Sambade, A., Doonan, J. H. and Lloyd, C. W. 2010, *New Phytol.*, 190, 258.
46. Cai, C., Li, Y., Shen, Y. and Ren, H. 2010, *Plant Signal. Behav.*, 5, 1619.
47. Klotz, J. and Nick, P. 2012, *New Phytol.*, 193, 576.
48. Dixit, R. and Cyr, R. 2004, *Plant Cell*, 16, 3274.
49. Allard, J. F., Wasteneys, G. O. and Cytrynbaum, E. N. 2010, *Mol. Biol. Cell*, 21, 278.
50. Eren, E. C., Dixit, R. and Gautam, N. 2010, *Mol. Biol. Cell*, 21, 2674.